Thermal Science and Engineering Progress 42 (2023) 101863

Contents lists available at ScienceDirect

Thermal Science and Engineering Progress

journal homepage: www.sciencedirect.com/journal/thermal-science-and-engineering-progress

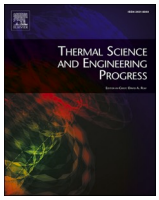

Thermo-kinetic analysis of pyrolysis of thermally pre-treated sewage sludge from the food industry

Aleksandra Petrovič [a,*], Janja Stergar [a], Lidija Škodič [a], Neža Rašl [a], Tjaša Cenčič Predikaka [b], Lidija Čuček [a], Darko Goričanec [a], Danijela Urbancl [a]

[a] Faculty of Chemistry and Chemical Engineering, University of Maribor, Smetanova ul. 17, 2000 Maribor, Slovenia
[b] IKEMA d.o.o., Institute for Chemistry, Ecology, Measurements and Analytics, Lovrenc na Dravskem polju 4, 2324 Lovrenc na Dravskem polju, Slovenia

ARTICLE INFO

Keywords:
Thermal pre-treatment
Pyrolysis
Industrial sewage sludge
Thermogravimetric analysis
Kinetic analysis
Thermodynamic analysis

ABSTRACT

Due to the specific characteristics of sewage sludge from the food industry, including its high fat content, its treatment is quite complex. Therefore, in this study, the effect of the pre-treatment processes torrefaction (T) and hydrothermal carbonization (HTC) on the pyrolysis of industrial sewage sludge (SS) from the vegetable oil industry was investigated by thermogravimetric analysis. Kinetic and thermodynamic analysis was performed using the Kissinger-Akahira-Sunose (KAS), Flynn-Wall-Ozawa (FWO), and Friedman (FRI) iso-conversional kinetic models. In addition, the influence of water replacement by whey in the hydrothermal carbonization process was investigated on the subsequent pyrolysis kinetics.

The activation energy (E_α) values for pyrolysis of industrial sewage sludge ranged from 49 to 372 kJ/mol. Pre-treatment (torrefaction, hydrothermal carbonization) of sewage sludge increases the activation energy significantly: the E_α values for torrefied (T-SS) and hydrothermally treated (HTC-SS) samples ranged from 177 to 689 kJ/mol and from 161 to 486 kJ/mol, respectively. The variations in activation energy and the generally lower activation energies for the HTC-SSW sample (158–445 kJ/mol) indicate that the use of whey in the HTC process affects the hydrochar properties and subsequent pyrolysis kinetics significantly. According to the results, the pre-treatment of the samples is reflected in better thermochemical properties and stability of the treated samples, as well as in the thermodynamic parameters of pyrolysis, since the pre-treated samples (especially the torrefied sample, T-SS) exhibited higher entropies and enthalpies and lower Gibbs free energies.

1. Introduction

The increasing population, development of civilisation and industrialisation have increased water consumption and the demand for clean water [1]. Since the discharge of wastewater degrades water quality and wastewater cannot be used directly for drinking water and industrial applications due to various pollutants, the treatment of domestic and industrial wastewater is needed urgently [2]. This leads to increased production of sewage sludge [3]. According to an EurEau briefing note, the total production of sewage sludge in Europe is about 8.7 Mt of dry solid/year [4], and it is still increasing.

Sewage sludge has a complex composition that depends greatly on the type of wastewater treated [5]. Various pollutants, such as heavy metals, pathogens and other toxic chemicals and hazardous substances accumulate in SS [6]. Therefore, SS can affect the environment and living organisms negatively if not treated properly. On the other hand, sewage sludge is a good source for energy recovery and production of fuels and chemicals [7]. Different types of sewage sludge can be distinguished, including municipal SS [8] and industrial SS [9], the latter often being more harmful to the environment because the content of toxic substances in industrial water is usually higher. Therefore, the conventional treatment methods, such as landfilling, soil application and composting cannot be applied to industrial SS [10]. For sustainable management of industrial sewage sludge, the development and investigation of alternative, cost-effective and environmentally acceptable treatment methods is crucial.

The increasing energy demand and rapid depletion of conventional fossil fuels [11] have accelerated the investigations on the production and use of alternative fuels [12] such as biodiesel [13], biogas [14], biochar [15] and hydrogen [16]. Several thermochemical processes have been applied successfully to produce biofuels and energy from SS, including combustion [17], gasification [18], supercritical water gasification [19], pyrolysis [20], torrefaction [21] and hydrothermal

* Corresponding author.
E-mail address: aleksandra.petrovic@um.si (A. Petrovič).

https://doi.org/10.1016/j.tsep.2023.101863
Received 27 January 2023; Received in revised form 19 April 2023; Accepted 20 April 2023
Available online 28 April 2023

Nomenclature

COD	Chemical oxygen demand
DTG_{max}	Maximal value of derivative curve
DM	Dry matter
FC	Fixed carbon
FWO	Flynn-Wall-Ozawa kinetic model
FRI	Friedman kinetic model
HHV	Higher heating value
HTC	Hydrothermal carbonization
ICP-OES	Inductively coupled plasma - optical emission spectrometry
KAS	Kissinger-Akahira-Sunose kinetic model
SS	Sewage sludge
SSW	Sewage sludge in combination with whey
T	Torrefaction
TGA	Thermogravimetric analysis
TOC	Total organic carbon
VFA	Volatile fatty acids
VM	Volatile matter
WWTP	Wastewater treatment plant
ΔH	Enthalpy
ΔG	Gibbs free energy
ΔS	Entropy
A	Pre-exponential factor
β	Heating rate
E_α	Activation energy
h	Planck constant ($6.626 \cdot 10^{-34}$ J·s)
K_B	Boltzmann constant ($1.381 \cdot 10^{-23}$J/K),
R	Universal gas constant (8.314 J/(mol·K))
T_p	Peak pyrolysis temperature (at DTG_{max})

carbonization [5].

Pyrolysis, i.e., thermal degradation at a temperature of > 400 °C in an inert atmosphere [22], is one of the most widely used thermal treatment processes for SS, as it reduces the volume of SS, destroys pathogens, immobilises toxic metals in the sludge, and offers the possibility of recovering fuels, energy and valuable chemicals from this waste [10]. The formation of the products (bio-oil, biochar and gases) depends strongly on the pyrolysis conditions, especially the pyrolysis temperature, and the energetic potential and properties of the pyrolysis products vary considerably [23]. Torrefaction, or mild pyrolysis, occurs at lower temperatures (200–300 °C), and produces a solid product with high energy density and enhanced physical properties [24].

Similar to torrefaction, hydrothermal carbonization (HTC) is carried out at low temperatures (180–350 °C), with the difference that it takes place at autogenous saturated vapour pressure, with hydrochar being the main product [25]. It has been shown that the addition of various catalysts, such as different acids and bases, salts, metal oxides, etc., improves carbonization during hydrothermal treatment [26]. The efficiency of hydrochar production and its physicochemical properties can also be improved by introducing microwave technology to heat the HTC reactor instead of conventional heating [27]. Otherwise, the main advantage of HTC treatment is the conversion of wet materials into solid carbonaceous material without pre-drying [28]. The solid product (biochar) obtained from HTC or pyrolysis can be used in various fields, such as fuel [6], fertiliser, or soil enhancer [29], biosorbent for water pollutants such as chlorine [27], dyes [30], heavy metals [31] and others.

In recent years, the combination of different treatment processes has gained attention because it offers several advantages. Pyrolysis has been combined successfully with processes such as anaerobic digestion [14], hydrothermal carbonization [32] and torrefaction [33]. The combination of HTC and pyrolysis brings benefits such as energy savings, improved quality of the products, i.e., oil, gas and char [32], and increased surface area and thermal stability of the char [3]. In addition, HTC pre-treatment can decrease the N and S content in the hydrochar [34], as well as affect NO_x emissions and heavy metal distribution during pyrolysis [25]. Similarly, a pre-treatment with torrefaction improves pyrolysis product properties [7], hydrochar production yield, and increases the overall energy efficiency [33].

The effects of torrefaction or HTC on subsequent thermochemical processing (pyrolysis, combustion) and product properties have previously been studied for various types of biomasses. For example, torrefaction was coupled with co-pyrolysis to enhance the properties of hydrochar from rice straw and oil sludge [33]. The effects of torrefaction's operating parameters on the kinetic behaviour of lignin samples in an oxidative atmosphere were investigated by Brillard et al. [24]. The impact of torrefaction on the pyrolysis of wheat straw and peanut stalks was explored in another study [35]. Several studies were dedicated to the pyrolysis of torrefied wood samples [36]. In contrast, the combination of torrefaction and pyrolysis is less common in the treatment of SS, although many studies addressed each process separately, including the study to investigate the torrefaction kinetics of SS [21], and the study to investigate the pyrolysis of SS to produce biochar for heavy metal sorption [37]. Kinetic studies of pyrolysis or combustion of torrefied SS are rare. One of the few studies investigated whether pre-treatment of SS with torrefaction in a fluidised bed reactor could improve the liquid pyrolysis product, i.e., oil [7], but the char properties were not investigated, indicating the need for additional research in this area.

In contrast to torrefaction, the impact of the HTC process on SS pyrolysis has been studied more intensively. Chen et. al. [34] studied the structural properties and reactivity of HTC-treated SS and the characteristics of the subsequent pyrolysis. The influence of HTC pre-treatment on the pyrolysis kinetics of SS and the effect of HTC on the devolatilisation and thermodynamic properties have been investigated elsewhere [38]. Wang et al. studied the pyrolysis of HTC-treated digestate of SS using a bench-scale pyrolyser [32], and Ma et al. investigated the thermodynamic characteristics of pyrolysis of hydrochars obtained from co-HTC of sawdust and SS [39]. The impact of HTC pre-treatment on the formation of polycyclic aromatic compounds during SS pyrolysis was investigated in another study [22].

Numerous studies have addressed the kinetic properties and thermodynamic behaviour of municipal SS during pyrolysis, but only a limited number of studies have focused on industrial SS, particularly from a thermodynamic perspective. The pyrolysis kinetics of activated sludge from petrochemical and oil refineries have been investigated [40], as well as those of pharmaceutical sludge [41], sludge from the food industry [42], sludge from a wastewater treatment plant (WWTP) in the chemical fibre industry [9], and sludge from the wood industry [43]. In another study, HTC pre-treated sludge from the wastewater treatment of a coal-methanol plant was subjected to pyrolysis [19]. Kinetic studies and kinetic data for pyrolysis of pre-treated SS from the vegetable oil industry are not found in the literature, which was one of the main reasons for conducting this study.

To improve the properties of products from thermochemical treatment of SS, the SS should be treated in combination with other types of biomass, due to its low volatile mater content. For SS co-pyrolysis, dry biomass feedstocks such as rice husks [44] and sawdust [45] are preferred, while wet biomass feedstocks such as manure, algae [46], olive pomace [47], and cheese whey [48] can be used for HTC. The use of cheese whey resulted in an improvement in the quality of the manure hydrochar, an acceleration of process reactions, and an enhancement in

nutrient recovery [48]. Due to its advantages, it could also be combined with SS. According to the available literature, the kinetics of pyrolysis of hydrochar obtained from the co-HTC of SS and cheese whey has not been studied yet.

Considering the above facts, and in order to fill the research gap in the pre-treatment of industrial SS, this study investigates the effects of pre-treatment processes, torrefaction and HTC on the pyrolysis kinetics of industrial SS obtained from a WWTP in the vegetable oil industry. In addition, the effects of replacing water with whey as the process liquid in the HTC process were investigated to study changes in the kinetics of the subsequent pyrolysis reaction. The kinetic and thermodynamic behaviour were investigated based on TGA measurements, using two integral iso-conversional methods (the KAS and FWO kinetic models) and one differential iso-conversional method (the FRI kinetic model).

Several novelties were introduced by this work. For the first time, the kinetic and thermodynamic parameters for the pyrolysis of SS hydrochar obtained from the co-carbonization (co-HTC) of industrial SS with whey were determined, and compared with those for the pyrolysis of SS hydrochar (obtained from water-based HTC) and SS biochar (obtained by torrefaction). What distinguishes this paper from the others is that two different pre-treatment methods were compared, providing a broader insight into the possible treatment of these industrial wastes and their use as fuel, while other works usually deal with a single process. In addition, the introduction of whey improved the fuel properties of SS hydrochar significantly.

2. Material and methods

The materials that were the subject of the experimental study are presented, the characterisation methods are described, and the pre-treatment procedure is explained in this section. The pyrolysis process of the samples and the TGA measurements are described, and the kinetic models are presented in addition.

2.1. Tested materials

The SS sample was collected from an industrial physico-chemical WWTP that treats wastewater generated from the production of edible vegetable oils and dressings. The sample contained 54.71 wt% of volatile matter, and was rich in fat (21.8 wt%), which made it suitable for energy recovery. The industrial SS sample was dried in a dryer at 40 °C, ground in a laboratory mill and stored in a closed container until the thermal treatment.

2.2. Pre-treatment of samples

The dried SS sample was pre-treated thermally by two different methods, torrefaction (T) and hydrothermal carbonization (HTC).

For the torrefaction pre-treatment, about 50 g of the sample was weighed into a ceramic pot covered with a ceramic lid and treated thermally at a temperature of 250 °C for 2 h in a laboratory furnace, EUP-K 6/1200 (manufacturer Bosio). The torrefaction was performed in two parallels. After completion of the torrefaction, the sample (named as "T-SS") was cooled and placed in the desiccator until used in the pyrolysis process and for characterisation.

The HTC process was executed in a non-stirred stainless steel hydrothermal autoclave reactor with a PPL liner with a volume of 300 mL. Two HTC experiments were performed. In the first one, 30 g of sewage sludge was mixed with 180 mL of distilled water (ratio 1:6, sample "HTC-SS"), while, in the second one, the distilled water was replaced by cheese whey (sample "HTC-SSW"), to study the influence of the type of process liquid on the hydrochar characteristics. The reactor with the prepared mixture was placed in an electric furnace and heated slowly to 250 °C (temperature interval 4 °C/min). The sample was exposed to hydrothermal carbonization for another 5 h. The duration of 5 h was chosen because previous laboratory experiments conducted with a duration of 2 h showed poor results in terms of carbonization. Each HTC experiment was repeated three times, to obtain enough sample for further analysis. After completion of the chemical reaction, the reactor was cooled and the solid phase was separated from the reaction liquid by vacuum filtration. The filtered process liquid was kept in a refrigerator until further testing. The hydrochar dried at 105 °C was later subjected to pyrolysis.

2.3. Pyrolysis and combustion

A thermogravimetric analyser (TGA/SDTA851e, Mettler Toledo), was used to perform pyrolysis and combustion of the studied samples in the temperature range of 30–900 °C. The pyrolysis process was conducted in an N_2 atmosphere (100 mL/min) at three different heating rates (β) of 10, 20 and 30 °C/min. The combustion of the samples was studied in an air atmosphere (100 mL/min), at a temperature interval of 30–900 °C and a heating rate of 20 °C/min. Three replicates of the TGA measurements were conducted for each heating rate, and the average values are shown in the graphs. The weight of the samples subjected to thermal degradation was approximately 23 ± 2 mg. In addition to the mass loss curves (TG curves), the derivative curves (DTG curves) were plotted of the mass loss.

2.4. Methods used for chemical characterisation of the samples

2.4.1. Characterisation of the solid samples

The solid samples (untreated and pre-treated SS) were characterised by proximate and ultimate analysis. To determine the ash content, the samples were combusted in a furnace at 800 °C (4 h), while the volatile matter (VM) was determined by combustion at 900 °C (1 h). The value of fixed carbon (FC) was determined as the difference (Eq. (1)):

$$FC\ (wt\%) = 100 - VM - Ash \tag{1}$$

The ultimate analysis (carbon, nitrogen, hydrogen and sulphur content) was executed by a PerkinElmer elemental analyser (Series II 2400), wherein the oxygen content was determined as follows (Eq. (2)):

$$O = 100 - C - H - N - S - Ash\ (all\ in\ wt\%) \tag{2}$$

The heavy metals in the SS were measured with the ICP-OES apparatus (inductively coupled plasma - optical emission spectrometry) [49]. The higher heating value (HHV) was determined using the IKA C6000 Isoperibol bomb calorimeter [50]. All of the above-mentioned analyses were performed in parallel. Fourier transform infrared (FTIR) spectra of the samples were recorded by a Shimadzu IRAffinity FTIR spectrophotometer using the KBr method for sample preparation (a sample pressed into tablet form).

2.4.2. Characterisation of the process liquid obtained in the HTC experiment

The process liquid obtained after hydrothermal carbonization (HTC) of the tested samples was characterised for total organic carbon – TOC [51], chemical oxygen demand – COD [52], and ammonium nitrogen (NH_4-N) content [53]. Conductivity and pH were determined using a WTW InoLab Multi 720 measuring instrument. Each process liquid was analysed in two parallel measurements.

2.5. The equations of the kinetic models

The kinetic study was performed using the differential iso-conversional method (Friedman model) and two integral iso-conversional methods (Kissinger-Akahira-Sunose and Flynn-Wall-Ozawa models) [54]. According to the literature [55], these three models are among the most commonly used iso-conversional models to describe the kinetic parameters of pyrolysis and biomass behaviour. The detailed description of the chosen kinetic models can be found in many previous works on pyrolysis kinetics, so only the final equations are

presented in this paper. The following equations (Eq.(3) - Eq.(5)) were used for the models KAS, FWO and FRI, respectively [54]:

$$\ln[\beta] = \ln\left[\frac{A \cdot E_\alpha}{R \cdot g(\alpha)}\right] - 5.331 - 1.052\frac{E_\alpha}{R \cdot T} \quad (3)$$

$$\ln\left[\frac{\beta}{T^2}\right] = \ln\left[\frac{R \cdot A}{E_\alpha \cdot g(\alpha)}\right] - \frac{E_\alpha}{R \cdot T} \quad (4)$$

$$\ln\left[\beta_i \cdot \left(\frac{d\alpha}{dT}\right)_{\alpha,i}\right] = \ln[A \cdot f(\alpha)] - \frac{E_\alpha}{R \cdot T_{\alpha,i}} \quad (5)$$

The next equation (Eq. (6) was used to calculate the pre-exponential factor (*A*) [56]:

$$A = \left[\beta \cdot E_\alpha \cdot exp\left(\frac{E_\alpha}{R \cdot T_p}\right)\right] \Big/ \left(R \cdot T_p^2\right) \quad (6)$$

The values of activation energy (E_α) were determined from the slope of the linear fitting plots of the models KAS, FWO and FRI constructed at a certain conversion point (α). The thermodynamic behaviour of the samples was described by the enthalpy ΔH (kJ/mol), the entropy ΔS (kJ/(mol·K)) and the Gibbs free energy ΔG(kJ/mol) (see Eq.(7) - Eq.(9)) [57]:

$$\Delta H = E_\alpha - RT_p \quad (7)$$

$$\Delta S = \frac{\Delta H - \Delta G}{T_p} \quad (8)$$

$$\Delta G = E_\alpha + R \cdot T_p \cdot \ln\left(\frac{K_B \cdot T_p}{h \cdot A}\right) \quad (9)$$

3. Results and discusion

First, the results of the chemical characterisation of untreated and thermally pre-treated samples are presented, followed by a discussion of the thermogravimetric behaviour of the samples subjected to pyrolysis and combustion, and comments on the kinetic and thermodynamic parameters calculated using the kinetic models KAS, FRI, and FWO, with emphasis on the effects of pre-treatment on the pyrolysis process.

3.1. Samples' characterisation

3.1.1. Characteristics of the untreated and pre-treated SS samples

The main characteristics of the untreated SS and the SS pre-treated by HTC and torrefaction are shown in Fig. 1.

The untreated SS contained 54.71 wt% of volatiles, 31.75 wt% of carbon (C) and a relatively high ash content of 42.29 wt%. The contents of Cd, Cr_{total}, Ni, Cu, Zn and Pb were 14.03, 63.01, 9.57, 11.87, 193.49 and 7.80 mg/kg DM, respectively. The pre-treatment increases the ash content and decreases the VM content, and also changes the elemental composition of the samples. Interestingly, only a little difference was observed in the results of ultimate and proximate analysis between the torrefied (T-SS sample) and the HTC-treated sample (HTC-SS). An exception was the sample HTC-SSW, where the process water was replaced by cheese whey, which, consequently, exhibited higher VM (51.19 wt%) and carbon content (35.47 wt%). This sample also had the highest heating value (HHV) among all the samples (18.25 MJ/kg, Fig. 1c). In general, thermo-chemical pre-treatment (torrefaction and HTC) of SS at low temperatures had little effect on HHV, as the values of the tested samples were quite similar (14.66 MJ/kg for the untreated SS sample, 14.72 MJ/kg for the T-SS and 14.24 MJ/kg for the HTC-SS sample). The sample HTC-SSW showed the most promising energy potential among all the tested materials due to the addition of whey. Otherwise, the HHV values of industrial SS were comparable to the HHV values of other types of SS, such as municipal SS (11.5–16.7 MJ/kg) [58], but lower than those of waste sludge from the food processing industry (19.53 MJ/kg) [42] and industrial sludge obtained from the treatment of wastewater from the chemical industry (20.94 MJ/kg) [19]. Pre-treatment (torrefaction or HTC) reduces the content of hydrogen and oxygen in the samples, which is reflected in a reduction of the H/C and O/C atomic ratios (Fig. 1d). The H/C ratios of the pre-treated samples were higher than those of the lignite, while the O/C ratios were lower. In the case of torrefaction, the oxygen and hydrogen contents were reduced, mainly by the release of water due to the dehydration reaction and the release of CO_2, CO, and light organic components [7], while, in the case of HTC, due mainly to the release of CO_2 because of the decarboxylation reaction [59].

Pre-treatment decreased the N content in the samples from 1.25 wt% (untreated SS) to 0.97 wt% (T-SS) and 0.55 wt% (HTC-SS), except for the

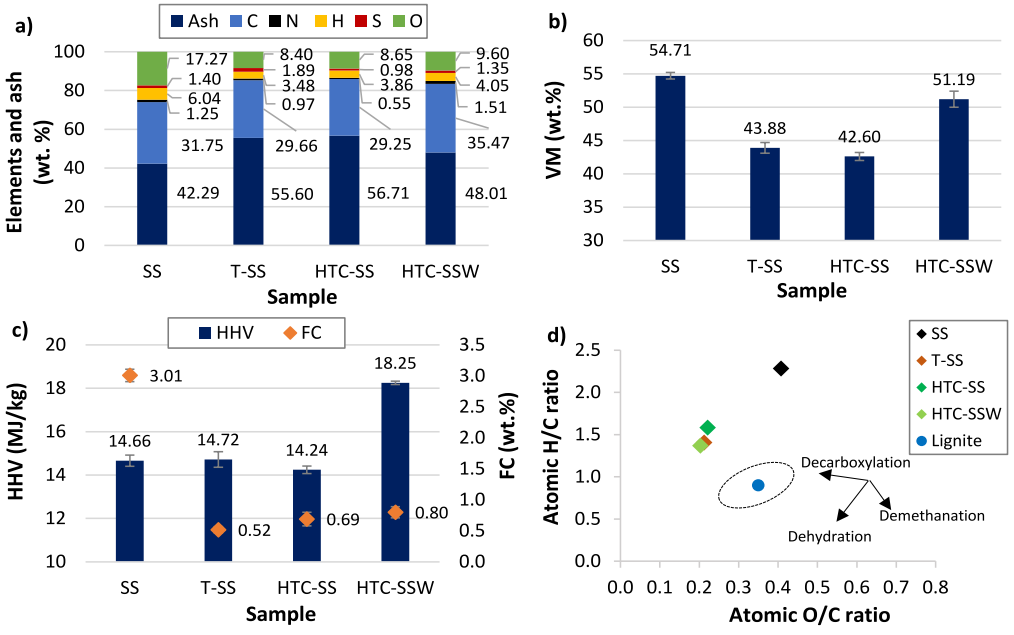

Fig. 1. Results of the characterisation of the solid samples: a) Elemental analysis and ash content, b) Volatile matter, c) HHV and fixed carbon, and d) Van Krevelen diagram (O/C and H/C atomic ratios).

sample HTC-SSW, where the value increased to 1.51 wt% because of the whey. The decrease in N content is connected with the degradation of proteins during pre-treatment [60]. The S content was in the range of 0.98–1.89 wt%. The torrefaction caused an increase of S in the char, while HTC treatment a decrease. The low N and S contents of hydrochar are favourable for its use as a fuel, as this can reduce the NO_X and SO_X formation during combustion [61].

The content of FC in the untreated SS was 3.01 wt%, while lower values were calculated for the pre-treated samples (<1 wt%). This behaviour was unusual, since other types of biomasses usually exhibited higher C and FC content after thermal treatment. However, SS is an exception, and the decrease of FC and carbon content in sewage sludge samples after thermal treatment was also observed in other studies [34].

Comparison of the FTIR spectra of the biochars obtained by pyrolysis with the spectra of the untreated and pre-treated SS (Fig. 2) shows significant changes in the chemical composition of these samples after thermal treatment. The untreated and torrefied samples contained functional groups typical of oils and waxes; fewer of these groups were detected in the HTC samples, while, in the pyrolysed samples, the peaks for these groups disappeared completely.

The untreated SS sample (Fig. 2a) shows a wide peak in the 3600–3100 cm^{-1} range corresponding to the vibrations of the (–OH) groups. The vibrations of the N–H groups of the amines and amides may also overlap in this area. The peaks at 2929 cm^{-1} and 2854 cm^{-1} correspond to the vibrations of aliphatic C–H bonds, and most likely represent fatty acids and saturated carbonaceous chains of oils [62]. The bands between 1800 and 1550 cm^{-1} represent the vibrations of the –C=O group of ketone, amide and carboxyl groups [59]. A wide peak at 1050 cm^{-1} and a peak at 600 cm^{-1} represent the Si–O vibrations of silicates [61] and Si–O–Al vibrations of alumina silicates [63].

The spectrum of the torrefied SS is very similar to the spectrum of untreated SS, except that the intensity of some peaks, such as the peak for the –OH groups, decreased due to the dehydration reaction during torrefaction. For the samples treated by the HTC method, the differences are even more obvious, as the peaks for the aliphatic C–H bonds, hydroxyl groups and ketone groups are lower, indicating that a decarboxylation reaction happened during the HTC treatment [59]. The absorption peaks of amine after the HTC treatment decreased in agreement with the hydrolysis of protein [60]. Besides, the peak at 550 cm^{-1} split into two peaks.

In the pyrolysed samples (Fig. 2b), the peaks of the aliphatic C–H bonds (2929 and 2854 cm^{-1}), hydroxyl groups (~3300 cm^{-1}), and ketone and amide groups of the proteins became weaker, and some of them had even disappeared. This indicates that most of the organic material in the samples had been decomposed and converted to bio-oil and biochar. The O- and N-containing compounds were converted to acids/esters and amines/amides in the bio-oil during pyrolysis, and later decarboxylation and deamination reactions took place as the pyrolysis temperature increased [34]. This may be the reason for the decrease in peak intensity of the nitrogen-containing groups in this study. The absorption peak of the C=C vibration of the aromatic ring, which reflects the presence of aromatic compounds in chars, appeared at about 1600 cm^{-1} [61,63].

The peaks at 1050, 600, and 550 cm^{-1}, representing various silicates and oxides (Si–O–Si, Si–O–Al, Mg–O, Fe–O, Al–O and others), became more pronounced and sharper after pyrolysis, especially in the case of the pyrolysed (pSS) and torrefied SS sample (pT-SS), as the ash content increased in the pyrolysed samples [60]. Interestingly, the peaks of the FTIR spectra of all SS samples pre-treated with HTC were less intense than the peaks of the other samples, which might be related to the fact that some organic components were already degraded during the HTC treatment and dissolved in the process liquids. These results indicate that the pre-treatment of the studied SS sample had a significant impact on the subsequent pyrolysis and the properties of the products.

The recorded FTIR spectra of SS from the edible oil industry had similar characteristics to those of the HTC-treated municipal SS [59,61] or pyrolysed SS [37] presented in other studies. The properties of the investigated samples, especially the sample HTC-SSW, indicate a promising potential for their further use for energy recovery in thermal treatment processes. However, due to the different structure and characteristics of the samples, the quality of the thermal treatment products may vary.

3.1.2. *The properties of the process liquids obtained from the HTC experiments*

The process liquids obtained from the HTC experiments were analysed for TOC, COD, NH_4-N content, conductivity and pH, the results of which are shown in Fig. 3.

The values of COD and TOC reflect the content of organic components, such as VFA (volatile fatty acids), alkenes, phenols and other components in the process liquids generated by the hydrolysis reaction during HTC treatment. As expected, the process liquid of the sample HTC-SSW exhibited higher values of TOC and COD than that of sample HTC-SS, due to the presence of cheese whey. For example, the sample HTC-SSW contained 55,523 mg/L COD (18,474 mg/L TOC), while the sample HTC-SS contained only 22,051 mg/L COD (7,050 mg/L TOC). The COD and TOC values of the process liquids obtained in this study were comparable to those obtained from the HTC of municipal SS [64]. Conductivity was also higher in the HTC-SSW sample, which could be due to higher ion concentrations in the liquid, since whey catalyses HTC reactions due to its acidic nature, and contributes to the release of nutrients [48].

The content of ammonia nitrogen was 513 mg/L for the sample HTC-SS and 1,810 mg/L for the sample HTC-SSW. The presence of N in the process liquids can be ascribed to the solubilisation and deamination of proteins during HTC [64]. Considerable amounts of N in the process liquids were also noticed in other studies on HTC treatment of municipal SS [15].

The pH of the process liquids was acidic. The pH of the HTC-SSW sample (5.41) was lower than that of the HTC-SS sample (5.49), which was due to the acids present in the whey. Otherwise, changes in pH depend on the presence of inorganic and organic compounds in the process liquids [65] caused by the solubilisation of ammonium, proteins, salts and other compounds. Volatile fatty acids such as acetic, propanoic and butyric acids, are also formed during the HTC process; they lower

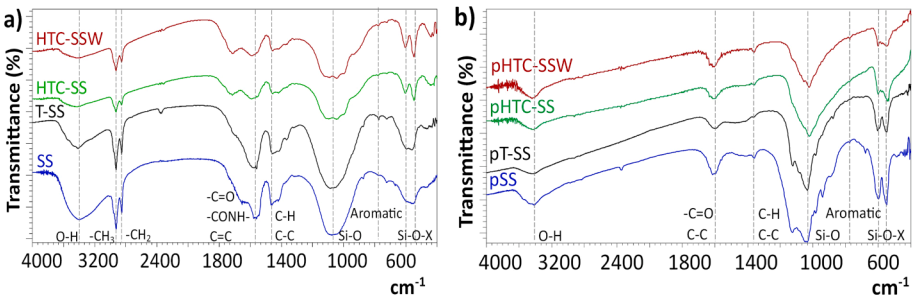

Fig. 2. FTIR spectra of a) Untreated and pre-treated samples and b) Pyrolysed samples.

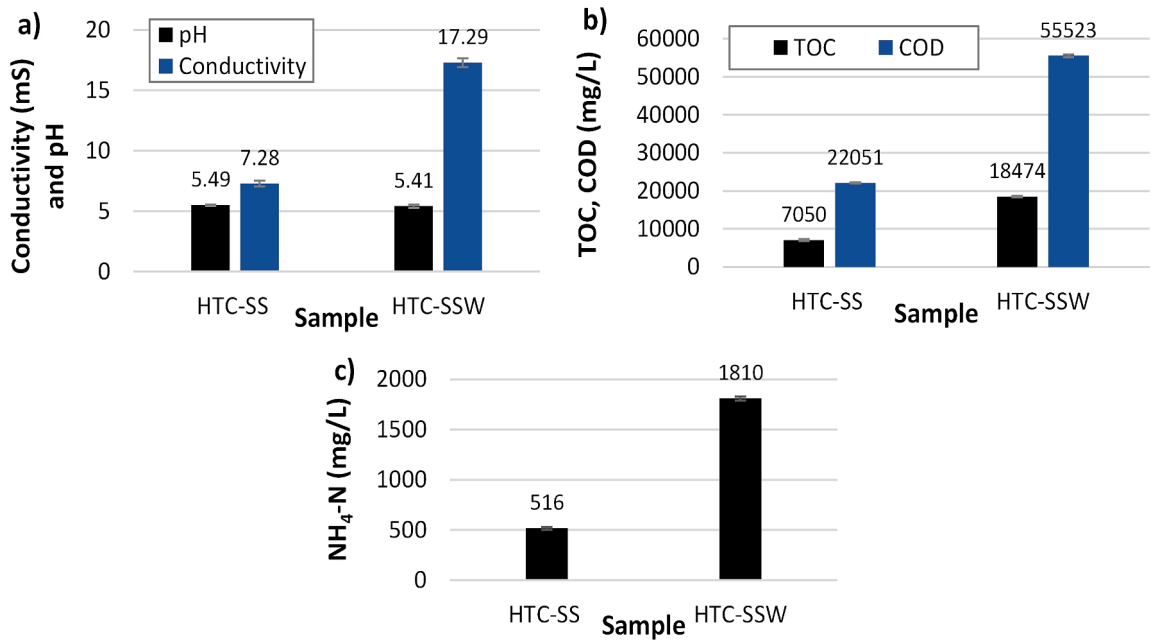

Fig. 3. Results of the characterisation of the process liquid from HTC experiments: a) Conductivity and pH, b) TOC and COD content and c) NH_4-N.

the pH value [64].

3.2. Thermogravimetric properties

3.2.1. Thermogravimetric behaviour of the samples during combustion and pyrolysis

The thermogravimetric (TG) and corresponding derivative (DTG) curves of SS, T-SS, HTC-SS and HTC-SSW samples exposed to pyrolysis (N_2 atmosphere) and the combustion process (air atmosphere) showed several differences in the thermogravimetric behaviour of these samples, including differences in mass loss, mass residue and peak pyrolysis temperature – T_p (see Fig. 4, Table S1).

The T_p of the DTG curves was higher for pyrolysis than for combustion. For example, for the torrefied sample (T-SS), the T_p of combustion was 240.3 °C and that of pyrolysis was 466.0 °C, so the peak temperature was shifted by ~ 225 °C for pyrolysis. This indicates that the main degradation in pyrolysis occurred at higher temperatures than in combustion. Similar results were observed for the untreated samples SS and HTC-SS, while a smaller difference was observed for the sample HTC-SSW. The shift of T_p to lower values under oxygen conditions was also noticed for SS treated with $FeCl_3$, which generates Fe_2O_3 upon heating, acting as a catalyst [66]. Since the industrial SS in this study also contained metal oxides, this could be one of the reasons for the T_p shift. Interestingly, in another study, the combustion of SS resulted in a higher T_p value than pyrolysis [67]. It can be concluded that the T_p is affected strongly by the chemical characteristics of SS. However, a higher mass loss was observed during combustion than during pyrolysis. The pre-treated samples lost 4–9 wt% more weight in combustion than in pyrolysis, with the largest difference observed for the HTC-SSW sample. The difference in weight loss was smaller for the untreated sample SS, only 1.5 wt%. In both processes, the weight loss of the pre-treated samples in the dehydration stage (temperatures up to 200 °C) was slower than that of the untreated SS, and the samples lost only a small amount of weight. The highest total weight loss in combustion was noticed for the untreated SS (56.74 wt%), followed by the samples HTC-SSW (51.96 wt%), HTC-SS (44.88 wt%) and T-SS (44.09 wt%). The lower percentage of mass loss of the pre-treated samples indicates that the pre-treated samples contained a lower proportion of combustible materials and more ash. In the pyrolysis, the weight loss for samples SS, T-SS, HTC-SS and HTC-SSW were 55.23, 41.37, 39.74 and 42.82 wt%, respectively.

The pre-treatment of the samples affected both processes, pyrolysis and combustion. The shape of the DTG curves of combustion of the HTC-treated SS samples differed significantly from those of the untreated SS

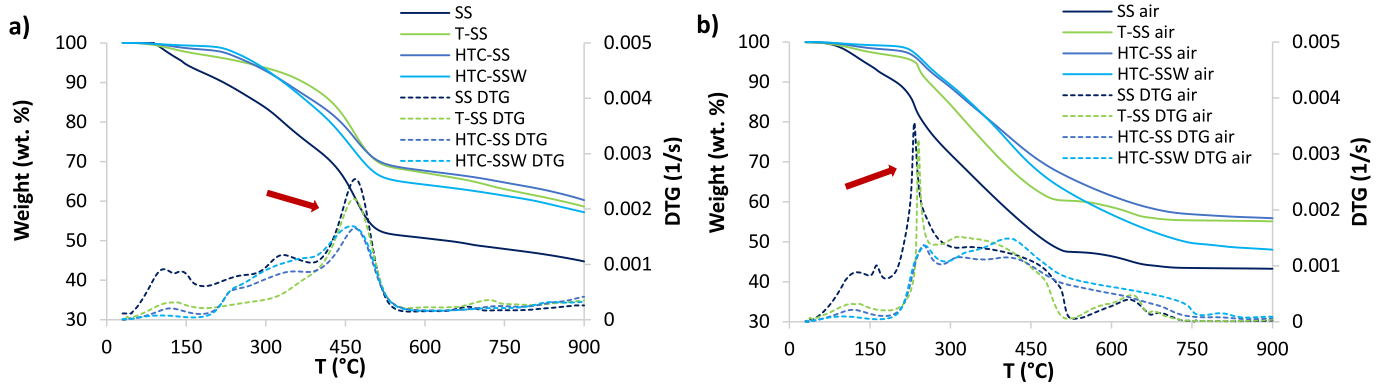

Fig. 4. Thermogravimetric curves and their first derivatives recorded for untreated and thermally pre-treated SS samples (T-SS, HTC-SS and HTC-SSW) subjected to: a) Pyrolysis (N_2 atmosphere) and, b) Combustion (air atmosphere).

and torrefied SS. The peak of the DTG curve (DTG_{max}) was much higher for the untreated SS and T-SS samples, reflecting the higher degradation rate of these samples during combustion. Similar could be assumed for pyrolysis. The combustion occurred in two main stages; the first peak at ~ 250 °C represents the combustion of light volatile matter (small organic molecules, cellulose and hemicellulose, amino acids) [15], while the broad peak at 350–500 °C represents the combustion of fixed carbon, i.e. heavy volatile components (lignin) [68].

Torrefaction pre-treatment has a greater influence on the pyrolysis of SS in the temperature interval between 175 and 400 °C (shoulder of the peak), while HTC pre-treatment has a greater effect on the behaviour of SS in the temperature interval of 400–580 °C, (DTG_{max} for the HTC-treated samples was below 1.8 1/s, while, for torrefied and untreated SS, it was above 2.2 1/s). The combustion of SS is affected highly by HTC pre-treatment, especially in the temperature range between 180 and 450 °C. The lower DTG peak of the HTC-treated samples was due to the higher ash content in the SS caused by the HTC treatment.

Pre-treatment had a relatively small impact on T_p in pyrolysis, while significant changes in T_p were observed in the HTC-treated samples during combustion. The differences in pyrolysis and combustion behaviour between the samples can be ascribed to the chemical changes caused by HTC and torrefaction pre-treatment, i.e., the removal of thermally less stable components from the SS due to aromatisation and carbonization [8]. The different duration of the pre-treatment, which was longer for HTC (5 h) than for torrefaction (2 h), may also affect the thermogravimetric behaviour of the samples.

3.2.2. *The effects of pre-treatment and heating rate on the pyrolysis of pre-treated samples*

The influences of pre-treatment and heating rate on the pyrolysis of pre-treated materials are shown in Fig. 5. The thermogravimetric curves of raw SS, torrefied SS (sample T-SS), and HTC-treated SS (samples HTC-SS and HTC-SSW) are shown at heating rates of 10, 20, and 30 °C/min. The thermogravimetric characteristics of TG and the DTG curves (weight loss in a given stage, peak temperature, DTG_{max}) are summarised in Table 1.

In general, the degradation of the samples occurred in three parts: dehydration (stage I), active pyrolysis (stage II), in which devolatilisation, decarboxylation, and carbonization occurred, and passive pyrolysis (stage III), in which thermal degradation happened of heavy fractions and inorganic components.

In the first stage (temperature interval of 30–180 °C), evaporation of the water occurred, i.e. dehydration reaction [10]. The highest weight loss was noticed in the pyrolysis of untreated SS (6.8–9.3 wt%). The other three samples showed much lower weight loss (<3 wt%) because the water was already released during the pre-treatment.

In the active pyrolysis (Stage II) that happened in the temperature interval between 180 and 580 °C, the most significant differences were observed in the DTG profiles, indicating a large influence of pre-treatment on the subsequent pyrolysis. Untreated SS in this stage lost ~ 42 wt% of weight, while pre-treated samples lost between 29 and 35 wt% (the sample HTC-SSW lost the highest mass percent and T-SS the lowest).

The active pyrolysis according to the DTG profile in the case of untreated SS, HTC-SS and HTC-SSW occurred in two parts: a) The temperature interval between 180 and 400 °C (a shoulder of the DTG peak) represents the degradation of carbohydrates and proteins, and b) The temperatures between 400 and 580 °C (the pronounced DTG peak) represent the degradation of lipids. According to the literature, the decomposition of lipids, i.e. fats, occurs between 200 and 600 °C [42], that of carbohydrates in the temperature range of 180–270 °C, and that of proteins between 180 and 350 °C [38]. Since the temperature ranges of decomposition of these components overlap, the individual peak for each component usually cannot be identified clearly. Although the samples HTC-SS and T-SS had relatively similar mass losses and peak pyrolysis temperatures, the shape of the DTG curves differed significantly in the temperature interval of 200–400 °C. The previously mentioned shoulder on the DTG curve was not observed in the case of

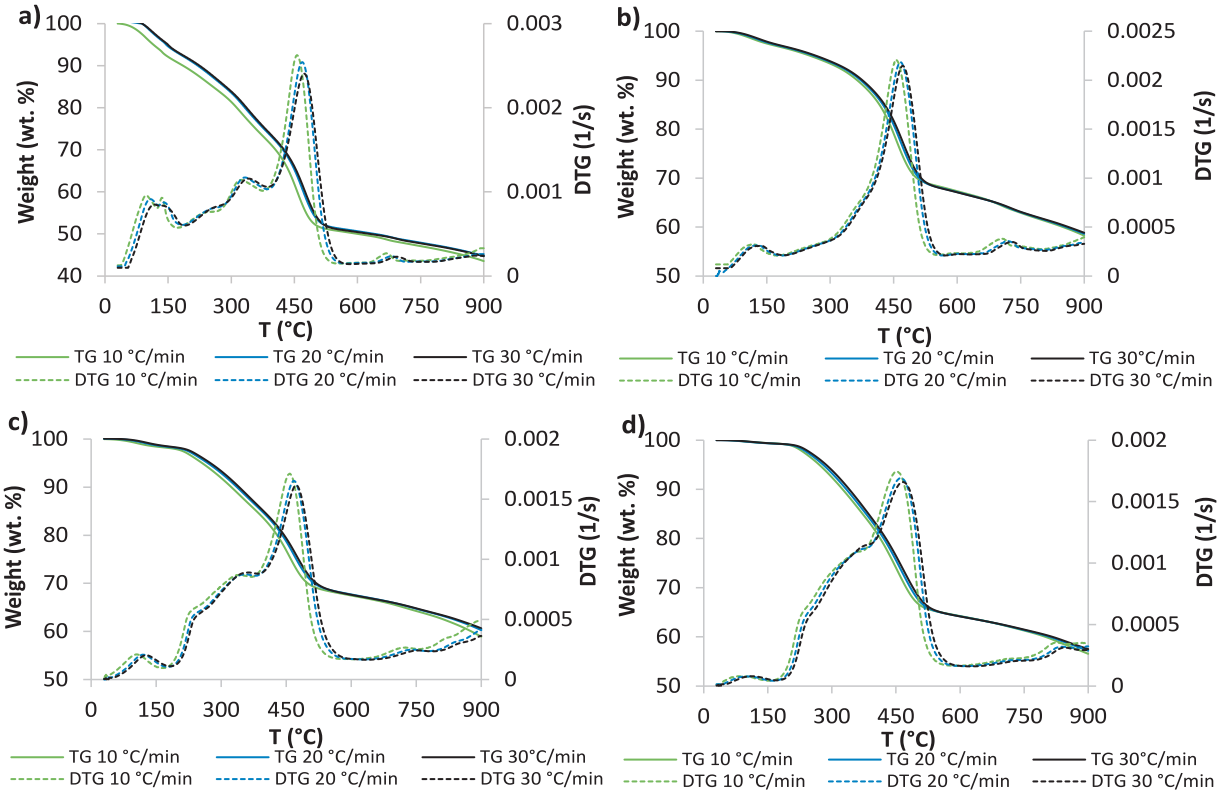

Fig. 5. TG and DTG curves of pyrolysis recorded at 10, 20 and 30 °C/min for the samples: a) SS, b) T-SS, c) HTC-SS and d) HTC-SSW.

Table 1
Characteristics of the thermogravimetric curves recorded during pyrolysis of the studied samples (weight loss, peak temperature, maximum value of the DTG curve).

Sample	Heating rate, β (°C/min)	Weight loss (wt%)			Total weight loss (wt%)	Residue (wt%)	T_p (°C)	DTG_{max} (1/s)
		Stage I	Stage II	Stage III				
SS	**10**	9.34 ± 0.26	40.33 ± 0.56	6.78 ± 0.15	56.46 ± 0.42	43.54 ± 0.42	456.3 ± 1.5	$2.62x10^{-3} \pm 2.3x10^{-5}$
	20	7.05 ± 0.80	42.01 ± 0.89	6.18 ± 0.31	55.23 ± 1.21	44.77 ± 1.21	469.0 ± 2.2	$2.54x10^{-3} \pm 0.9x10^{-5}$
	30	6.86 ± 0.15	42.43 ± 1.03	6.01 ± 0.06	55.30 ± 0.38	44.70 ± 0.38	473.0 ± 0.8	$2.40x10^{-3} \pm 4.4x10^{-5}$
T-SS	**10**	3.04 ± 0.07	29.16 ± 0.67	9.55 ± 0.44	41.75 ± 0.85	58.25 ± 0.85	456.2 ± 1.4	$2.20x10^{-3} \pm 1.8x10^{-5}$
	20	2.84 ± 0.11	29.57 ± 0.52	8.96 ± 0.12	41.37 ± 0.72	58.63 ± 0.72	466.0 ± 1.0	$2.18x10^{-3} \pm 7.6x10^{-5}$
	30	2.70 ± 0.21	29.75 ± 0.34	8.70 ± 0.56	41.16 ± 0.14	58.84 ± 0.14	471.0 ± 0.3	$2.15x10^{-3} \pm 4.8x10^{-5}$
HTC-SS	**10**	1.80 ± 0.09	30.39 ± 1.21	8.91 ± 0.03	41.10 ± 0.88	58.90 ± 0.88	458.7 ± 2.6	$1.71x10^{-3} \pm 2.1x10^{-5}$
	20	1.59 ± 0.05	30.37 ± 0.47	7.78 ± 0.39	39.74 ± 0.23	60.26 ± 0.23	467.7 ± 1.9	$1.65x10^{-3} \pm 0.7x10^{-5}$
	30	1.49 ± 0.14	30.53 ± 0.11	7.34 ± 0.08	39.36 ± 0.65	60.64 ± 0.65	473.0 ± 3.1	$1.61x10^{-3} \pm 1.1x10^{-5}$
HTC-SSW	**10**	0.71 ± 0.13	34.73 ± 0.67	8.02 ± 0.64	43.45 ± 0.09	56.55 ± 0.09	453.2 ± 0.5	$1.74x10^{-3} \pm 3.7x10^{-5}$
	20	0.75 ± 0.06	34.75 ± 0.88	7.32 ± 0.27	42.82 ± 1.04	57.18 ± 1.04	461.3 ± 0.8	$1.69x10^{-3} \pm 5.6x10^{-5}$
	30	0.73 ± 0.04	34.78 ± 0.26	6.99 ± 0.19	42.50 ± 0.56	57.50 ± 0.56	466.5 ± 2.7	$1.66x10^{-3} \pm 0.5x10^{-5}$

sample T-SS. This can be ascribed to differences in chemical composition, indicating that these components were completely degraded by torrefaction (during torrefaction, the sample SS underwent the devolatilisation and carbonization process), but only partially by the HTC process, although both types of pre-treatment were performed at the same temperature (250 °C). Besides, the residence time in the HTC pre-treatment was even longer than in the torrefaction. During HTC pre-treatment, most likely only easily degradable components (carbohydrates) were removed, while more stable substances (proteins, lipids, lignin) were apparently not devolatilised completely. The formation of secondary char by the Maillard reaction [3], which is thermally more stable, could be another explanation.

In the last stage (III), i.e., passive pyrolysis, the samples lost another 6–9 wt% in weight, due mainly to the decomposition of heavy components into low-molecular weight substances [33]. The differences between the samples were smaller. A peak at 700–750 °C was related to the decomposition of minerals, since the decomposition of organic components essentially finishes below 600 °C [69]. The total weight loss of the samples SS, T-SS, HTC-SS and HTC-SSW ranged from 43.54 to 44.77 wt %, 58.25–58.84 wt%, 58.90–60.64 wt% and 56.55–57.50 wt%, respectively. The replacement of process water with whey in the HTC process (HTC-SSW) resulted in an increase in weight loss during active pyrolysis, as well as an increase in the total weight loss. In addition, the peak temperature in this sample decreased slightly compared to the sample HTC-SS. Otherwise, the samples pre-treated with HTC showed a similar shape of the TG pyrolysis curves.

The heating rates tested had a relatively low impact on the pyrolysis of the tested samples. Only a slight increase in peak temperature was observed. For example, the peak temperature of sample T-SS increased from 456 °C (at 10 °C/min) to 471 °C (at 30 °C/min). Similarly, the weight loss and DTG_{max} changed slightly. The shorter reaction time at higher heating rate delayed the peak of the DTG curves, resulting in an increase in peak temperature [70]. This was due to changes in heat transfer between the particles, as the efficiency of heat transfer may decrease with increasing the heating rate [41]. On the other hand, an insufficient heat supply due to a lower heating rate may hinder the reaction kinetics, cause side reactions and reduce the reaction rate [44]. A relatively small effect of the heating rate on pyrolysis and weight loss was also found in the study on the pyrolysis of municipal SS [71].

3.3. Kinetic analysis of pyrolysis based on the FWO, KAS and FRI models

The following subsections present the results of the kinetic analysis performed on the thermogravimetric results of TG and DTG curves of untreated, torrefied and HTC pre-treated SS recorded at 10, 20 and 30 °C/min (see Fig. 5).

3.3.1. Activation energy

The activation energies (E_α) for pyrolysis of untreated SS, torrefied SS and HTC pre-treated SS (samples HTC-SS and HTC-SSW), determined using the KAS, FWO, and FRI models, are shown in Fig. 6. The values were calculated from the slope of the linear trend lines (constructed for conversion levels of 0.1–0.8 in 0.1 steps) shown in Fig. S1. At higher conversion levels the results diverged, and low correlation factors were observed, most likely due to the higher ash content in the samples affecting the reactions. The error bars in the graphs indicate the confidence intervals (95% confidence level).

The activation energy (E_α) represents the energy barrier that the material must overcome to release the volatile compounds from the biomass [55]. In other words, it is the energy necessary to start the chemical reaction [72]. Quite different E_α profiles were noticed for the studied samples, with the pre-treated SS samples having higher E_α values than the untreated one during the entire conversion process, which can be assigned to the pre-treatment. In general, the reaction with higher E_α requires a higher reaction temperature and longer time for completion of the thermal decomposition [73]. For all samples, a significant increase in E_α was observed at lower conversion levels (<0.4), while the increase was less at higher conversions, although E_α was strongly dependent on the nature of the sample. Thus, the activation energies were influenced strongly by the conversion rate. The variability of E_α with α was related to the nature and extent of the reaction, particularly structural changes and the multistep reaction nature of thermal degradation [74].

The E_α values of the untreated SS (Fig. 6a) increased from 49 kJ/mol ($\alpha = 0.1$) to 326 kJ/mol at $\alpha = 0.6$, and then remained almost in the same range until the conversion level of $\alpha = 0.8$. The highest E_α value for untreated SS was 372 kJ/mol. The activation energies at lower conversions are related to moisture release, while, at higher conversions the increase in E_α is ascribed to the gradual decrease in volatile matter and the increase of char formation [44]. Theoretically, E_α usually varies between 40 and 300 kJ/mol [55], although higher values have been reported for industrial sludges (see Table 2): for SS from the chemical industry between 170 and 593 kJ/mol [43], for SS from the wood industry in the range of 125–756 kJ/mol [43], for pharmaceutical sludge between 114 and 552 kJ/mol [41], and for SS from the food industry between 69 and 683 kJ/mol [42]. Otherwise, a significant change in E_α (increase/decrease) reflects that the reactions occur in parallel or sequentially, while a constant E_α reflects a one-step reaction during material decomposition [75]. The increase in E_α at high conversions may be due to the decomposition of char formed during polycondensation, side-chain cyclisation, or crosslinking of polymer carbons [39].

The E_α values of the torrefied SS (Fig. 6b) were much higher, ranging from 177 to 689 kJ/mol. For comparison, in one of the few studies that focused on the pyrolysis kinetics of the torrefaction of SS, the E_α values for torrefied municipal SS were also high, in the range of 220–914 kJ/mol [68]. However, significant variations in E_α were observed during the pyrolysis of torrefied SS, as, after an initial increase in E_α up to a conversion level of $\alpha = 0.3$, a slight decrease was noticed, but, later, at $\alpha = 0.7$, the values again increased sharply. The increase in E_α at higher conversion levels could be attributed to the lignin decomposition and

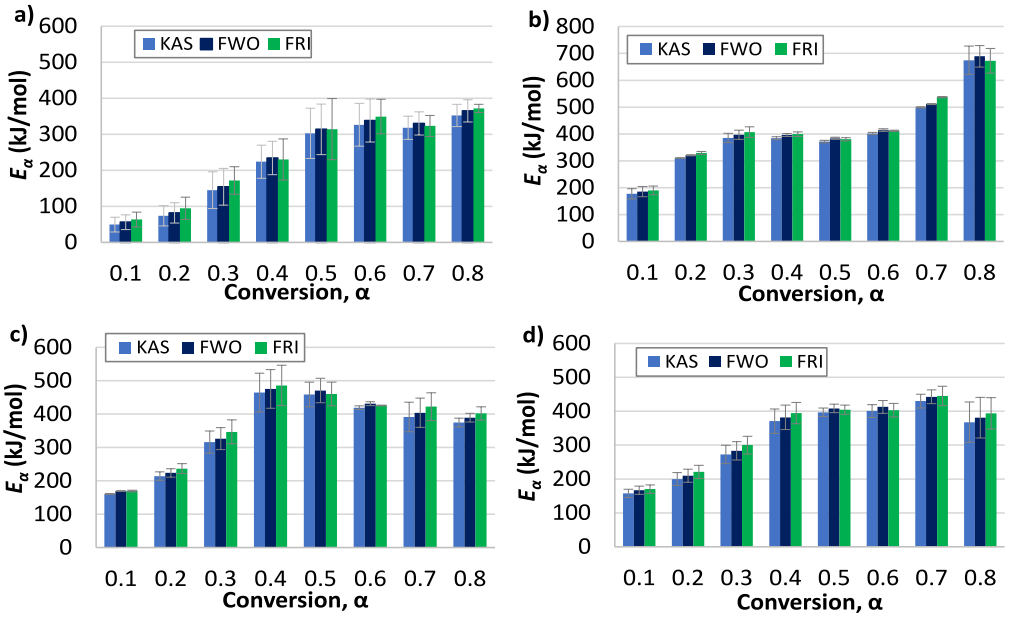

Fig. 6. E_α as a function of conversion level calculated with the models KAS, FWO and FRI for the samples: a) SS, b) T-SS, c) HTC-SS and d) HTC-SSW.

Table 2
Comparison of results of kinetic studies on pyrolysis of industrial SS and other types of SS.

Material	E_α (kJ/mol)	A (1/s)	ΔH(kJ/mol)	ΔG(kJ/mol)	ΔS(J/(mol·K))	Kinetic model	Ref.
Industrial SS	49–372	$1.03x10^{01}$–$3.96x10^{24}$	43–366	209–222	(−242)–(210)	FWO, KAS, FRI	This study
T-SS	177–689	$4.45x10^{10}$–$2.71x10^{47}$	171–683	205–213	(−57)–(647)		
HTC-SS	161–486	$2.69x10^{09-6}$.$62x10^{32}$	155–480	208–214	(−80)–(368)		
HTC-SSW	158–445	$1.97x10^{09}$–$1.51x10^{30}$	152–439	206–212	(−83)–(317)		
Municipal SS	41–167	$2.12x10^{01}$– $4.85x10^{13}$	36–163	161–167	(–233)–(4)	FWO	[78]
SS digestate	66–351	$6.73x10^{03}$–$3.80x10^{30}$	61–347	160–168	(−185)–(327)		
Municipal SS	63–323	$3.22x10^{04}$– $5.78x10^{26}$	70–318	85–90	(−90)–(650)	FWO	[56]
Municipal SS	46–232	$1.02x10^{09}$– $3.97x10^{19}$	41–227	53–295	(−151)–(63)	FWO	[77]
Municipal SS	100–300	/	/	/	/	KAS, FRI, FWO	[71]
Municipal SS	195–563	$1.64\ x10^{18}$–$2.96\ x10^{49}$	186–545	126–131	90–688	KAS, FWO	[41]
Pharmaceutical sludge	114–552	$1.93\ x10^{12}$–$4.79\ x10^{52}$	111–547	90–125	−24–(749)		
SS–chemical industry	170–593	/	/	/	/	Distributed activation energy model	[43]
SS–wood industry	125–756	/	/	/	/		
SS–food industry	69–683	$9.7\ x10^{05}$–$5.0\ x10^{67}$	65–677	130–140	−134–(991)	FWO, KAS, Starink	[42]
Paper mill sludge	140–163	$1.03x10^{09}$–$3.01x10^{13}$	/	/	/	Coats-Redfern	[69]
Textile dyeing sludge	80–200	$2.53x10^{07}$–$8.74x10^{16}$	/	/	/		
Municipal SS	213–531	$4.49\ x10^{46}$	307	155	270	FWO, KAS	[39]
HTC-SS	123–298	$5.79\ x10^{21}$	216	181	53		
Sawdust (SD)	168–181	$2.88\ x10^{12}$	168	183	–23		
HTC-SD	181–189	$1.46x10^{13}$	179	185	−8.49		
Municipal SS*	113–184	$8.77x10^{11}$–$1.91x10^{21}$	/	/	/	FWO	[70]
HTC-SS*	136–287	$7.85\ x10^{15}$–$7.58x10^{29}$	/	/	/		
Municipal SS	45–390	$3.97x10^{03}$–$4.69x10^{33}$	/	/	/	Distributed activation energy model	[34]
HTC-SS	30–160	$2.91x10^{02}$–$5.79x10^{31}$	/	/	/		
Municipal SS	167–245	$9.44x10^{15}$–$9.33x10^{23}$	163–233	155–156	25–160	FWO, KAS, FRI, Starink	[38]
HTC-SS	98–214	$2.1x10^{06}$–$4.0x10^{15}$	90–203	205–210	−171–(-3)		
Municipal SS	140–260	/	/	/	/	KAS	[68]
T-SS	220–914	/	/	/	/		
Wheat straw (WS)	69–357	$9.67x10^{03}$–$9.10\ x10^{29}$	64–352	165–173	−183 – (315)	FWO	[35]
T-WS	51–256	$1.52x10^{02}$– $4.66x10^{20}$	46–251	169–177	−217 – (1 3 7)		
Wood biomass (WB)*	51–205	$5.43x10^{06}$–$1.64\ x10^{16}$	/	/	/	FWO, KAS, FRI	[74]
T-WB*	20–275	$3.77x10^{04}$– $2.21x10^{22}$	/	/	/		

*Values reported for the combustion.

the degradation of other high-temperature stable components. These components act as barriers during carbonization, and hinder the heat diffusion and the release of volatiles, which is reflected in an increased E_α [35]. In addition, the ash contained in the sample may cover the pores of the residue, and increase the difficulty of the reaction, resulting in a significant increase in E_α [44].

This is related to the chemical structure of the T-SS sample. The torrefied sample exhibited better thermal stability, which was also confirmed by the increase in T_p, so a higher activation energy is required for its degradation. The increase in activation energy and thermal stability after pre-treatment of biomass with the torrefaction process was also observed in the study on corncobs [76], lignin [24] and other similar materials. In contrast, some researchers reported the opposite effect, e.g., torrefaction of peanut stalks and wheat straw reduced the E_α of subsequent pyrolysis [35]. This effect was also noticed in HTC-treated SS [39], which is in contrast to the present study, because the E_α values

of the HTC-SS and HTC-SSW samples were higher than those of the untreated SS.

The E_α values of the SS changed significantly after HTC pre-treatment (Fig. 6c). The E_α values for HTC-SS ranged from 161 to 486 kJ/mol, and those of the sample HTC-SSW (Fig. 6d) ranged from 158 to 445 kJ/mol. The E_α profile of the sample HTC-SSW was similar to that of the sample HTC-SS. The E_α values of the sample HTC-SS increased up to the 0.4 conversion level, while they decreased slowly above it. The decrease was a consequence of the facilitated release of volatiles due to the porous structure of the intermediates formed during pyrolysis, the increased surface area of the hydrochars, and the catalysis of the inherent metals [77]. In addition, the E_α values are affected strongly by the pre-treatment temperature [6]. Otherwise, an increase in the pyrolysis E_α of HTC-treated samples (compared to untreated samples) was due to the formation of aromatic structures during the HTC pre-treatment, which reduced the degree of disorder of carbon layers in the SS and led to the formation of thermodynamically stable products [3].

Comparison of the E_α values calculated in this study shows close agreement with those reported in other studies (see Table 2). However, it must be taken into account that the type and characteristics of SS are different. The E_α values for pre-treated samples (HTC-treated and torrefied) were generally higher than the values reported in the literature.

All three kinetic models produced comparable E_α values, although the Friedman model gave slightly higher E_α values than the FWO model, which also showed higher values than the KAS model. The variations in the E_α results between the models are a consequence of the differences in the equations of the kinetic models. Nevertheless, all three methods were accurate in their calculations. The goodness of fit, i.e., the correlation coefficients (R^2) of the linear fit plots for E_α using the KAS model for the untreated SS ranged from 0.88 to 0.99, for sample T-SS from 0.94 to 1.00, and for samples HTC-SS and HTC-SSW > 0.98 (see Fig. S1 and Table S2), reflecting the credibility of the results.

3.3.2. Pre-exponential factor and kinetic compensation effect

The values of the pre-exponential factor (A), which describes the chemistry of the solid phase pyrolysis reaction [57], are listed in Table S2. A also represents the number of collisions between reactants during thermal degradation [72]. The values of A followed the trend of E_α, as their values increased or decreased proportionally. The pre-treated samples had higher A values than untreated SS (for all three kinetic models), wherein the highest A values were calculated for the torrefied sample SS, while the HTC treated samples gave lower, but quite similar, values. A varied between $1.03\text{x}10^{01}$-$3.96\text{x}10^{24}$ 1/s for untreated SS, $4.45\text{x}10^{10}$–$2.71\text{x}10^{47}$ 1/s for T-SS, $2.69\text{x}10^{09}$–$6.62\ \text{x}10^{32}$ 1/s for HTC-SS, and $1.97\text{x}10^{09}$–$1.51\text{x}10^{30}$ 1/s for HTC-SSW. The variation of A with α (degree of conversion) is related to the composition of the material and the degradation reactions. The pre-exponential factors of the pre-treated samples were higher than 10^9 1/s for all conversion levels, which is due to the formation of a loose (simple) complex, indicating a low degradation rate and a high energy requirement for decomposition [75]. The complexity of the pyrolysis reaction of the pre-treated samples was already confirmed by changes in E_α, as these samples exhibited higher E_α. The A values below 10^9 1/s in the case of the untreated SS indicate a surface reaction in which a closed (tight junctional) complex was formed and degradation occurred in a simpler manner. The values that ranged from 10^4 to 10^{18} 1/s reflect the first-order factor range [79]. The wide range of A values indicates the heterogeneous nature of the pyrolysis reaction and the complex multistep degradation mechanism of the studied materials, especially the pre-treated samples. The pre-exponential factors calculated in this study are close to those of municipal SS and other types of SS, which are listed in Table 2.

The kinetic compensation effect characterising the relationship between A and the E_α values at a specific conversion level is shown for the studied samples in Fig. S2. The following linear relationship holds: $lnA = aE_\alpha + b$, where a and b represent constants related to the compensation coefficients [54]. The lowest correlation for the kinetic compensation effect was observed for the HTC-SS sample (0.89), while the HTC-SSW and T-SS samples had better correlations. The best correlation was observed for the untreated SS sample ($R^2 > 0.98$).

3.4. Thermodynamic analysis

Based on the results of the kinetics analysis, the thermodynamic parameters of pyrolysis were calculated (for this purpose, the peak temperatures of the DTG curves obtained at a heating rate of 20 °C/min were used). The profiles of entropy (ΔS) are shown in Fig. 7, and the values of enthalpy (ΔH) and Gibbs free energy (ΔG) in Table S2.

3.4.1. The entropy (ΔS)

Entropy (ΔS) reflects the disorder of matter and energy in a system [57]. As shown in Fig. 7, pre-treatment affected the ΔS values significantly. For the untreated SS, the values obtained with the FWO model ranged from −231 to 201 J/(mol·K), with negative values characteristic up to a conversion degree of 0.3; thereafter, the values became positive, and increased with the conversion level and temperature. Similar to the other kinetic parameters, the pre-treated samples exhibited higher ΔS values. The increase in ΔS reflects an increase in the difficulty of the reaction [76]. The torrefied sample T-SS exhibited the highest ΔS values among all samples, as the values calculated with the FWO model ranged from −45 to 647 J/(mol·K). A negative value for this sample was observed only at a conversion level of 0.1. This confirms the findings about the complexity of torrefaction and its multistage mechanism [35].

For the HTC-treated SS samples (HTC-SS and HTC-SSW) the values were negative up to a conversion level of 0.2. The ΔS values calculated with the FWO model varied between −68 and 354 J/(mol·K) for the sample HTC-SS, and between −70 and 314 J/(mol·K) for the sample HTC-SSW. The results of the other two kinetic models were close to these values. For the HTC-SS sample, the ΔS values decreased at higher conversion levels (>0.4), while they remained in the same range for the HTC-SSW sample.

The phenomenon of occurrence of both positive and negative ΔS values reflects the complexity of the thermal degradation process [56]. A positive ΔS value indicates that the disorder of the products is greater than that of the reactants due to bond dissociation, and that the system is not in thermal equilibrium. On the other hand, negative ΔS values indicate that the system is near thermal equilibrium [73]. Therefore, low ΔS values reflect that the activated system has a more ordered structure than the raw material and a considerable amount of free energy [75]. Similar trends in ΔS values have been observed in other studies (see Table 2) on municipal SS and HTC pre-treated SS [38] and SS from the food industry [42], where a wide range of ΔS values have been reported,

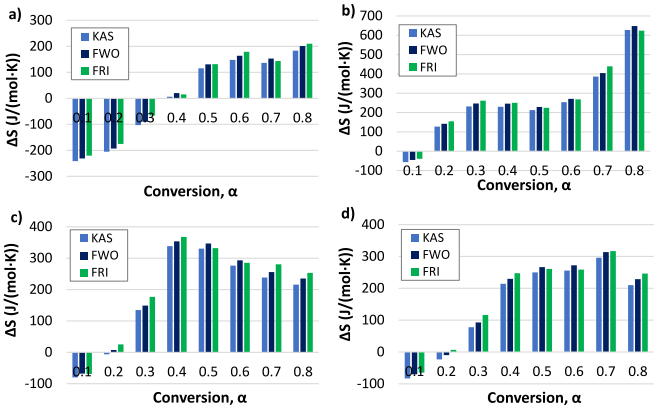

Fig. 7. ΔS values as a function of the conversion level, calculated with the models KAS, FWO and FRI for the samples: a) SS, b) T-SS, c) HTC-SS and d) HTC-SSW.

indicating the complexity of the decomposition of these materials.

3.4.2. Changes in enthalpy (ΔH) *and Gibbs free energy* (ΔG)

The parameter ΔH designates whether energy is lost or acquired during the conversion of material into products [75], and thus provides information about the endothermic or exothermic nature of the reaction. In pyrolysis, ΔH refers to the total energy consumed in the conversion of biomass into biochar, bio-oil and biogas [79]. The ΔH values presented in Table S2 show the same tendency as the E_α values. The positive ΔH values for all samples and at all conversion levels indicate that the thermo-chemical degradation of the tested materials was not spontaneous (i.e., it was an endothermic reaction), requiring heat input from the environment into the system. Knowledge of the ΔH value of the pyrolysis process is important for the design of the thermal degradation process and predicting its efficiency [35]. Different profiles, i.e., variations of ΔH with the degree of conversion, indicate that the pre-treated samples differ in composition, even though they originate from the same SS. The untreated sample SS had lower enthalpies than the pre-treated SS, so it required less energy for thermal degradation than the other three samples. The difference between E_α and ΔH was about 6 kJ/mol for all three models. A small difference between these two parameters designates favourable conditions for the formation of the activated complex, and suggests that there is a very low energy barrier for the formation of the products. For the torrefied and HTC-treated samples, a significant increase in ΔH was observed at conversion levels below 0.4, indicating that a high amount of energy was required for their degradation in this range. This is due mainly to the decomposition of thermally stable components. The ΔH values calculated here agree well with literature data (see Table 2).

The parameter ΔG, also known as free enthalpy, shows an elevation in the energy of the pyrolysis reaction during the formation of the activated complexes [79]. The ΔG of the untreated SS was in the range of 209–222 kJ/mol (Table S2), while, for the pre-treated samples (T-SS, HTC-SS and HTC-SSW) slightly lower energies were observed in a narrower range, between 205 and 214 kJ/mol. Values between 90 and 125 kJ/mol were reported for pharmaceutical sludge, between 155 and 156 kJ/mol for municipal SS, and in the range of 205–210 kJ/mol for HTC-treated SS [38]. Since ΔG reflects the spontaneity of the reaction and the amount of available internal energy [56], the relatively high internal energy of the studied samples indicates their potential for energy recovery. In general, the results of the kinetic and thermodynamic analyses revealed that the tested samples can be used as fuel. The chemical analyses confirmed that the pre-treatment improves the thermal stability and fuel properties of the industrial SS.

4. Conclusions

The kinetic of pyrolysis of pre-treated industrial SS from the vegetable oil industry was investigated, using torrefaction and HTC as the pre-treatment methods. The influence of water replacement by whey was also investigated as a process liquid in the HTC process on further pyrolysis.

The pre-treatment (torrefaction, HTC) of the samples changed their thermogravimetric behaviour in the pyrolysis process, as the shape of the TG and DTG curves differed, although the pre-treated samples had relatively similar mass losses and peak temperatures. The replacement of water with whey in hydrothermal carbonization (HTC) improved the fuel properties of the hydrochar, and obviously affected the pyrolysis kinetics. The highest HHV (18.25 MJ/kg) and C content (35.47 wt%) were measured in this sample. Kinetic and thermodynamic analyses performed using the KAS, FWO, and FRI kinetic models generally showed higher E_α, ΔS, and ΔH values for the pre-treated samples than for untreated SS, with the highest values observed for the torrefied sample, followed by the HTC-treated samples. For pyrolysis of the untreated, torrefied and HTC-treated SS samples, entropies (ΔS) varied between −241 and 210, −57 and 647, and between −80 and 368 J/(mol·K), respectively. The HTC-treated sample with whey as the process liquid gave comparable results, with the values ranging from −83 to 317 J/(mol·K). Chemical analysis of the process waters from HTC treatment showed that they can be used in anaerobic digestion processes due to their high TOC and COD content.

The limitation of this study is that the pyrolysis experiments were performed on a small amount of samples in a TGA analyser and only the characteristics of the solid product were studied, which is only a basis for further investigations. In order to obtain a complete insight into the pyrolysis of the selected materials and the effects of pre-treatment, the experiments should be performed on a larger scale, and all products should be investigated, including the gaseous and liquid (oil) phases. However, the results obtained provide a good basis for further studies, and are useful for waste management planning in the vegetable oil industry. Further studies could be related to the investigation of the effects of the minerals in the sewage sludge ash on the pyrolysis process, the optimisation of the process parameters and further use and modification of the products.

Declaration of Competing Interest

The authors declare that they have no known competing financial interests or personal relationships that could have appeared to influence the work reported in this paper.

Data availability

Data will be made available on request.

Acknowledgment

The authors thank the Slovenian Research Agency for financial support (core funding for research P2-0421 and P2-0046). We would also like to thank the company IKEMA d.o.o. for their help in carrying out the chemical analyses.

Appendix A. Supplementary data

Supplementary data to this article can be found online at https://doi.org/10.1016/j.tsep.2023.101863.

References

[1] A. Panagopoulos, Techno-economic assessment and feasibility study of a zero liquid discharge (ZLD) desalination hybrid system in the Eastern Mediterranean, Chem. Eng. Process.: Process Intensif. 178 (2022) 109029.
[2] A. Panagopoulos, Brine management (saline water & wastewater effluents): Sustainable utilization and resource recovery strategy through Minimal and Zero Liquid Discharge (MLD & ZLD) desalination systems, Chem. Eng. Process.: Process Intensif., 176 (2022) 108944, 10.1016/j.cep.2022.108944.
[3] L. Wang, Y. Chang, A. Li, Hydrothermal carbonization for energy-efficient processing of sewage sludge: A review, Renew. Sust. Energ. Rev. 108 (2019) 423–440, https://doi.org/10.1016/j.rser.2019.04.011.
[4] EurEau, Waste water treatment – sludge management, Briefing note on sludge management, (2021), https://www.eureau.org/resources/briefing-notes/5629-briefing-note-on-sludge-management/file.
[5] R.D.V.K. Silva, Z. Lei, K. Shimizu, Z. Zhang, Hydrothermal treatment of sewage sludge to produce solid biofuel: Focus on fuel characteristics, Bioresour. Technol. Rep. 11 (2020), 100453, https://doi.org/10.1016/j.biteb.2020.100453.
[6] S. Paiboonudomkarn, K. Wantala, Y. Lubphoo, R. Khunphonoi, Conversion of sewage sludge from industrial wastewater treatment to solid fuel through hydrothermal carbonization process, Mater. Today: Proc. 75 (2023) 85–90, https://doi.org/10.1016/j.matpr.2022.11.107.
[7] M. Atienza-Martínez, I. Fonts, L. Lázaro, J. Ceamanos, G. Gea, Fast pyrolysis of torrefied sewage sludge in a fluidized bed reactor, Chem. Eng. J. 259 (2015) 467–480, https://doi.org/10.1016/j.cej.2014.08.004.
[8] R. Wang, C. Wang, Z. Zhao, J. Jia, Q. Jin, Energy recovery from high-ash municipal sewage sludge by hydrothermal carbonization: Fuel characteristics of biosolid products, Energy 186 (2019), 115848, https://doi.org/10.1016/j.energy.2019.07.178.
[9] S. Xie, G. Yu, C. Li, J. Li, G. Wang, S. Dai, Y. Wang, Treatment of high-ash industrial sludge for producing improved char with low heavy metal toxicity, J. Anal. Appl. Pyrolysis 150 (2020), 104866, https://doi.org/10.1016/j.jaap.2020.104866.

[10] S. Tang, C. Zheng, F. Yan, N. Shao, Y. Tang, Z. Zhang, Product characteristics and kinetics of sewage sludge pyrolysis driven by alkaline earth metals, Energy 153 (2018) 921–932, https://doi.org/10.1016/j.energy.2018.04.108.
[11] Y. Shen, A review on hydrothermal carbonization of biomass and plastic wastes to energy products, Biomass Bioenergy 134 (2020), 105479, https://doi.org/10.1016/j.biombioe.2020.105479.
[12] N. Jaat, A. Khalid, F. Yaahaya, I. Shahridzuan Abdullah, S.F.Z. Abidin, B. Manshoor, I. Zaman, A. Sapit, H. Koten, Effects of organic and pyrolysis fuel on ignition and combustion process, Int. J. Nanoelectron. Mater. 15 (2022) 545–553.
[13] R. Saputra Nursal, A. Khalid, I. Shahridzuan Abdullah, N. Jaat, N. Darlis, H. Koten, Autoignition behavior and emission of biodiesel from palm oil, waste cooking oil, tyre pyrolysis oil, algae and jatropha, Fuel, 306 (2021) 121695, 10.1016/j.fuel.2021.121695.
[14] Q. Feng, Y. Lin, Integrated processes of anaerobic digestion and pyrolysis for higher bioenergy recovery from lignocellulosic biomass: A brief review, Renew. Sust. Energ. Rev. 77 (2017) 1272–1287, https://doi.org/10.1016/j.rser.2017.03.022.
[15] G. Shan, W. Li, S. Bao, Y. Li, W. Tan, Co-hydrothermal carbonization of agricultural waste and sewage sludge for product quality improvement: Fuel properties of hydrochar and fertilizer quality of aqueous phase, J. Environ. Manage. 326 (2023), 116781, https://doi.org/10.1016/j.jenvman.2022.116781.
[16] S. Eckart, R. Prieler, C. Hochenauer, H. Krause, Application and comparison of multiple machine learning techniques for the calculation of laminar burning velocity for hydrogen-methane mixtures, Therm. Sci. Eng. Prog. 32 (2022), 101306, https://doi.org/10.1016/j.tsep.2022.101306.
[17] P.J. Arauzo, M. Atienza-Martínez, J. Ábrego, M.P. Olszewski, Z. Cao, A. Kruse, Combustion Characteristics of Hydrochar and Pyrochar Derived from Digested Sewage Sludge, Energies 13 (2020) 4164, https://doi.org/10.3390/en13164164.
[18] A. Zachl, A. Soria-Verdugo, M. Buchmayr, J. Gruber, A. Anca-Couce, R. Scharler, C. Hochenauer, Stratified downdraft gasification of wood chips with a significant bark content, Energy 261 (2022), 125323, https://doi.org/10.1016/j.energy.2022.125323.
[19] P. Lv, R. Wu, J. Wang, Y. Bai, L. Ding, J. Wei, X. Song, G. Yu, Energy recovery of livestock manure and industrial sludge by co-hydrocarbonisation coupled to pyrolysis and gasification, J. Clean. Prod. 374 (2022), 133996, https://doi.org/10.1016/j.jclepro.2022.133996.
[20] Y. Tang, M.S. Alam, K.O. Konhauser, D.S. Alessi, S. Xu, W. Tian, Y. Liu, Influence of pyrolysis temperature on production of digested sludge biochar and its application for ammonium removal from municipal wastewater, J. Clean. Prod. 209 (2019) 927–936, https://doi.org/10.1016/j.jclepro.2018.10.268.
[21] Q. Nguyen, D.D. Nguyen, H. Vothi, C. He, M. Goodarzi, Q.-V. Bach, Isothermal torrefaction kinetics for sewage sludge pretreatment, Fuel 277 (2020), 118103, https://doi.org/10.1016/j.fuel.2020.118103.
[22] T. Liu, Y. Guo, N. Peng, Q. Lang, Y. Xia, C. Gai, Q. Zheng, Z. Liu, Identification and quantification of polycyclic aromatic hydrocarbons generated during pyrolysis of sewage sludge: Effect of hydrothermal carbonization pretreatment, J. Anal. Appl. Pyrolysis 130 (2018) 99–105, https://doi.org/10.1016/j.jaap.2018.01.021.
[23] C. Figueiredo, H. Lopes, T. Coser, A. Vale, J. Busato, N. Aguiar, E. Novotny, L. Canellas, Influence of pyrolysis temperature on chemical and physical properties of biochar from sewage sludge, Arch. Agron. Soil Sci. 64 (2018) 881–889, https://doi.org/10.1080/03650340.2017.1407870.
[24] A. Brillard, G. Trouvé, P. Maryandyshev, D. Kehrli, V. Lyubov, J.F. Brilhac, Analysis through thermogravimetric analyses of the impact of torrefaction processes performed under a non-oxidative atmosphere on hydrolysis lignin samples, Fuel 260 (2020), 116261, https://doi.org/10.1016/j.fuel.2019.116261.
[25] T. Liu, Z. Liu, Q. Zheng, Q. Lang, Y. Xia, N. Peng, C. Gai, Effect of hydrothermal carbonization on migration and environmental risk of heavy metals in sewage sludge during pyrolysis, Bioresour. Technol. 247 (2018) 282–290, https://doi.org/10.1016/j.biortech.2017.09.090.
[26] O.S. Djandja, R.K. Liew, C. Liu, J. Liang, H. Yuan, W. He, Y. Feng, B.G. Lougou, P.-G. Duan, X. Lu, S. Kang, Catalytic hydrothermal carbonization of wet organic solid waste: A review, Sci. Total Environ. 873 (2023), 162119, https://doi.org/10.1016/j.scitotenv.2023.162119.
[27] P.N.Y. Yek, R.K. Liew, W.A. Wan Mahari, W. Peng, C. Sonne, S.H. Kong, M. Tabatabaei, M. Aghbashlo, Y.-K. Park, S.S. Lam, Production of value-added hydrochar from single-mode microwave hydrothermal carbonization of oil palm waste for de-chlorination of domestic water, Sci. Total Environ., 833 (2022) 154968, 10.1016/j.scitotenv.2022.154968.
[28] M. Breulmann, M. van Afferden, R.A. Müller, E. Schulz, C. Fühner, Process conditions of pyrolysis and hydrothermal carbonization affect the potential of sewage sludge for soil carbon sequestration and amelioration, J. Anal. Appl. Pyrolysis 124 (2017) 256–265, https://doi.org/10.1016/j.jaap.2017.01.026.
[29] S. Celletti, A. Bergamo, V. Benedetti, M. Pecchi, F. Patuzzi, D. Basso, M. Baratieri, S. Cesco, T. Mimmo, Phytotoxicity of hydrochars obtained by hydrothermal carbonization of manure-based digestate, J. Environ. Manage. 280 (2021), 111635, https://doi.org/10.1016/j.jenvman.2020.111635.
[30] W. Tu, Y. Liu, Z. Xie, M. Chen, L. Ma, G. Du, M. Zhu, A novel activation-hydrochar via hydrothermal carbonization and KOH activation of sewage sludge and coconut shell for biomass wastes: Preparation, characterization and adsorption properties, J. Colloid Interface Sci. 593 (2021) 390–407, https://doi.org/10.1016/j.jcis.2021.02.133.
[31] Y. Chen, M. Li, Y. Li, Y. Liu, Y. Chen, H. Li, L. Li, F. Xu, H. Jiang, L. Chen, Hydroxyapatite modified sludge-based biochar for the adsorption of Cu^{2+} and Cd^{2+}: Adsorption behavior and mechanisms, Bioresour. Technol. 321 (2021), 124413, https://doi.org/10.1016/j.biortech.2020.124413.
[32] S. Wang, H. Persson, W. Yang, P.G. Jönsson, Pyrolysis study of hydrothermal carbonization-treated digested sewage sludge using a Py-GC/MS and a bench-scale pyrolyzer, Fuel 262 (2020), 116335, https://doi.org/10.1016/j.fuel.2019.116335.
[33] H. Xu, S. Cheng, D. Hungwe, K. Yoshikawa, F. Takahashi, Co-pyrolysis coupled with torrefaction enhances hydrocarbons production from rice straw and oil sludge: The effect of torrefaction on co-pyrolysis synergistic behaviors, Appl. Energy 327 (2022), 120104, https://doi.org/10.1016/j.apenergy.2022.120104.
[34] R. Chen, S. Yuan, X. Wang, X. Dai, Y. Guo, C. Li, H. Wu, B. Dong, Mechanistic insight into the effect of hydrothermal treatment of sewage sludge on subsequent pyrolysis: Evolution of volatile and their interaction with pyrolysis kinetic and products compositions, Energy 266 (2023), 126330, https://doi.org/10.1016/j.energy.2022.126330.
[35] B. Gajera, U. Tyagi, A.K. Sarma, M.K. Jha, Impact of torrefaction on thermal behavior of wheat straw and groundnut stalk biomass: Kinetic and thermodynamic study, Fuel Communications 12 (2022), 100073, https://doi.org/10.1016/j.jfueco.2022.100073.
[36] A.C. Louwes, L. Basile, R. Yukananto, J.C. Bhagwandas, E.A. Bramer, G. Brem, Torrefied biomass as feed for fast pyrolysis: An experimental study and chain analysis, Biomass Bioenergy 105 (2017) 116–126, https://doi.org/10.1016/j.biombioe.2017.06.009.
[37] J. Fan, Y. Li, H. Yu, Y. Li, Q. Yuan, H. Xiao, F. Li, B. Pan, Using sewage sludge with high ash content for biochar production and Cu(II) sorption, Sci. Total Environ. 713 (2020), 136663, https://doi.org/10.1016/j.scitotenv.2020.136663.
[38] W. Liu, X. Zheng, Z. Ying, Y. Feng, B. Wang, B. Dou, Hydrochar prepared from municipal sewage sludge as renewable fuels: Evaluation of its devolatilization performance, reaction mechanism, and thermodynamic property, J. Environ. Chem. Eng. 10 (2022), 108339, https://doi.org/10.1016/j.jece.2022.108339.
[39] J. Ma, H. Luo, Y. Li, Z. Liu, D. Li, C. Gai, W. Jiao, Pyrolysis kinetics and thermodynamic parameters of the hydrochars derived from co-hydrothermal carbonization of sawdust and sewage sludge using thermogravimetric analysis, Bioresour. Technol. 282 (2019) 133–141, https://doi.org/10.1016/j.biortech.2019.03.007.
[40] X. Yang, Z. Jiang, Kinetic studies of overlapping pyrolysis reactions in industrial waste activated sludge, Bioresour. Technol. 100 (2009) 3663–3668, https://doi.org/10.1016/j.biortech.2009.03.002.
[41] H. Liu, G. Xu, G. Li, Pyrolysis characteristic and kinetic analysis of sewage sludge using model-free and master plots methods, Process Saf. Environ. Prot. 149 (2021) 48–55, https://doi.org/10.1016/j.psep.2020.10.044.
[42] G.R. Mong, W.W.F. Chong, S.A.M. Nor, J.-H. Ng, C.T. Chong, R. Idris, J. Too, M. C. Chiong, M.A. Abas, Pyrolysis of waste activated sludge from food manufacturing industry: Thermal degradation, kinetics and thermodynamics analysis, Energy 235 (2021), 121264, https://doi.org/10.1016/j.energy.2021.121264.
[43] G. Liu, H. Song, J. Wu, Thermogravimetric study and kinetic analysis of dried industrial sludge pyrolysis, Waste Manage. 41 (2015) 128–133, https://doi.org/10.1016/j.wasman.2015.03.042.
[44] C. Wang, H. Bi, Q. Lin, X. Jiang, C. Jiang, Co-pyrolysis of sewage sludge and rice husk by TG–FTIR–MS: Pyrolysis behavior, kinetics, and condensable/non-condensable gases characteristics, Renew. Energy 160 (2020) 1048–1066, https://doi.org/10.1016/j.renene.2020.07.046.
[45] H.-J. Huang, T. Yang, F.-Y. Lai, G.-Q. Wu, Co-pyrolysis of sewage sludge and sawdust/rice straw for the production of biochar, J. Anal. Appl. Pyrolysis 125 (2017) 61–68, https://doi.org/10.1016/j.jaap.2017.04.018.
[46] C.I. Aragón-Briceño, A.K. Pozarlik, E.A. Bramer, L. Niedzwiecki, H. Pawlak-Kruczek, G. Brem, Hydrothermal carbonization of wet biomass from nitrogen and phosphorus approach: A review, Renew. Energy 171 (2021) 401–415, https://doi.org/10.1016/j.renene.2021.02.109.
[47] M. Gimenez, M. Rodríguez, L. Montoro, F. Sardella, G. Rodríguez-Gutierrez, P. Monetta, C. Deiana, Two phase olive mill waste valorization, Hydrochar production and phenols extraction by hydrothermal carbonization, Biomass Bioenergy 143 (2020), 105875, https://doi.org/10.1016/j.biombioe.2020.105875.
[48] Y.Z. Belete, V. Mau, R. Yahav Spitzer, R. Posmanik, D. Jassby, A. Iddya, N. Kassem, J.W. Tester, A. Gross, Hydrothermal carbonization of anaerobic digestate and manure from a dairy farm on energy recovery and the fate of nutrients, Bioresour. Technol., 333 (2021) 125164, 10.1016/j.biortech.2021.125164.
[49] EN 16170:2016, Sludge, treated biowaste and soil - Determination of elements using inductively coupled plasma optical emission spectrometry (ICP-OES), (2016), https://ecommerce.sist.si/catalog/standards/cen/c359e442-fd27-4e82-830e-318685e45172/en-16170-2016.
[50] SIST-TS CEN/TS 16023:2014, Characterization of waste - Determination of gross calorific value and calculation of net calorific value, (2014), https://ecommerce.sist.si/catalog/standards/sist/011369fc-bfbb-4f6d-8322-9d041a122efc/sist-ts-cen-ts-16023-2014.
[51] SIST EN 1484:1998, Water analysis - Guidelines for the determination of total organic carbon (TOC) and dissolved organic carbon (DOC), (1998), https://ecommerce.sist.si/catalog/standards/sist/6e87b67f-9039-481c-ad82-0c82fc31e997/sist-en-1484-1998.
[52] SIST ISO 6060:1996, Water quality – Determination of the chemical oxygen demand, (1996), https://ecommerce.sist.si/catalog/standards/sist/3e03c177-0a23-470f-94d4-4761ce418e30/sist-iso-6060-1996.
[53] ISO 5664:1984, Water quality — Determination of ammonium — Distillation and titration method, (1984), https://www.iso.org/standard/11757.html.
[54] Z. Yao, S. Yu, W. Su, W. Wu, J. Tang, W. Qi, Kinetic studies on the pyrolysis of plastic waste using a combination of model-fitting and model-free methods, Waste Manage. Res. 38 (2020) 77–85, https://doi.org/10.1177/0734242X19897814.
[55] S. Sobek, S. Werle, Kinetic modelling of waste wood devolatilization during pyrolysis based on thermogravimetric data and solar pyrolysis reactor

performance, Fuel 261 (2020), 116459, https://doi.org/10.1016/j.fuel.2019.116459.
[56] A. Zaker, Z. Chen, M. Zaheer-Uddin, J. Guo, Co-pyrolysis of sewage sludge and low-density polyethylene – A thermogravimetric study of thermo-kinetics and thermodynamic parameters, J. Environ Chem. Eng. 104554 (2020), https://doi.org/10.1016/j.jece.2020.104554.
[57] S.R. Naqvi, Z. Hameed, R. Tariq, S.A. Taqvi, I. Ali, M.B.K. Niazi, T. Noor, A. Hussain, N. Iqbal, M. Shahbaz, Synergistic effect on co-pyrolysis of rice husk and sewage sludge by thermal behavior, kinetics, thermodynamic parameters and artificial neural network, Waste Manage. 85 (2019) 131–140, https://doi.org/10.1016/j.wasman.2018.12.031.
[58] M. Ma, D. Xu, Y. Zhi, W. Yang, P. Duan, Z. Wu, Co-pyrolysis re-use of sludge and biomass waste: Development, kinetics, synergistic mechanism and industrialization, J. Anal. Appl. Pyrolysis 168 (2022), 105746, https://doi.org/10.1016/j.jaap.2022.105746.
[59] C. Wang, W. Zhu, X. Fan, Char derived from sewage sludge of hydrothermal carbonization and supercritical water gasification: Comparison of the properties of two chars, Waste Manage. 123 (2021) 88–96, https://doi.org/10.1016/j.wasman.2021.01.027.
[60] X. Zhuang, Y. Huang, Y. Song, H. Zhan, X. Yin, C. Wu, The transformation pathways of nitrogen in sewage sludge during hydrothermal treatment, Bioresour. Technol. 245 (2017) 463–470, https://doi.org/10.1016/j.biortech.2017.08.195.
[61] Y.-Q. Shan, X.-Q. Deng, R. Luque, Z.-X. Xu, L. Yan, P.-G. Duan, Hydrothermal carbonization of activated sewage sludge over ammonia-treated Fenton sludge to produce hydrochar for clean fuel use, Green Chem. 22 (2020) 5077–5083, https://doi.org/10.1039/D0GC01701A.
[62] A. Boukerroui, L. Belhocine, S. Ferroudj, Regeneration and reuse waste from an edible oil refinery, Environ. Sci. Pollut. Res. 25 (2018), https://doi.org/10.1007/s11356-017-9971-8.
[63] C. Zheng, X. Ma, Z. Yao, X. Chen, The properties and combustion behaviors of hydrochars derived from co-hydrothermal carbonization of sewage sludge and food waste, Bioresour. Technol. 285 (2019), 121347, https://doi.org/10.1016/j.biortech.2019.121347.
[64] M. Langone, D. Basso, Process Waters from Hydrothermal Carbonization of Sludge: Characteristics and Possible Valorization Pathways, Int. J. Environ. Res. Public Health 17 (2020) 6618. https://www.mdpi.com/1660-4601/17/18/6618.
[65] C.I. Aragón-Briceño, O. Grasham, A.B. Ross, V. Dupont, M.A. Camargo-Valero, Hydrothermal carbonization of sewage digestate at wastewater treatment works: Influence of solid loading on characteristics of hydrochar, process water and plant energetics, Renew. Energy 157 (2020) 959–973, https://doi.org/10.1016/j.renene.2020.05.021.
[66] M.B. Folgueras, M. Alonso, R.M. Díaz, Influence of sewage sludge treatment on pyrolysis and combustion of dry sludge, Energy 55 (2013) 426–435, https://doi.org/10.1016/j.energy.2013.03.063.
[67] A. Magdziarz, S. Werle, Analysis of the combustion and pyrolysis of dried sewage sludge by TGA and MS, Waste Manage. 34 (2014) 174–179, https://doi.org/10.1016/j.wasman.2013.10.033.
[68] M. Li, H. Wang, Z. Huang, X. Yuan, M. Tan, L. Jiang, Z. Wu, X. Qin, H. Li, Comparison of atmospheric pressure and gas-pressurized torrefaction of municipal sewage sludge: Properties of solid products, Energy Convers. Manage. 213 (2020), 112793, https://doi.org/10.1016/j.enconman.2020.112793.
[69] S. Feng, G. Zhang, D. Yuan, Y. Li, Y. Zhou, F. Lin, Co-pyrolysis of paper mill sludge and textile dyeing sludge with high calorific value solid waste: Pyrolysis kinetics, products distribution, and pollutants transformation, Fuel 329 (2022), 125433, https://doi.org/10.1016/j.fuel.2022.125433.
[70] T. Liu, Q. Lang, Y. Xia, Z. Chen, D. Li, J. Ma, C. Gai, Z. Liu, Combination of hydrothermal carbonization and oxy-fuel combustion process for sewage sludge treatment: Combustion characteristics and kinetics analysis, Fuel 242 (2019) 265–276, https://doi.org/10.1016/j.fuel.2019.01.035.
[71] N. Miskolczi, S. Tomasek, Investigation of Pyrolysis Behavior of Sewage Sludge by Thermogravimetric Analysis Coupled with Fourier Transform Infrared Spectrometry Using Different Heating Rates, Energies 15 (2022) 5116. https://www.mdpi.com/1996-1073/15/14/5116.
[72] S.R. Naqvi, I. Ali, S. Nasir, S. Ali Ammar Taqvi, A.E. Atabani, W.-H. Chen, Assessment of agro-industrial residues for bioenergy potential by investigating thermo-kinetic behavior in a slow pyrolysis process, Fuel, 278 (2020) 118259, 10.1016/j.fuel.2020.118259.
[73] S. Rasam, A. Moshfegh Haghighi, K. Azizi, A. Soria-Verdugo, M. Keshavarz Moraveji, Thermal behavior, thermodynamics and kinetics of co-pyrolysis of binary and ternary mixtures of biomass through thermogravimetric analysis, Fuel, 280 (2020) 118665, 10.1016/j.fuel.2020.118665.
[74] R. Barzegar, A. Yozgatligil, H. Olgun, A.T. Atimtay, TGA and kinetic study of different torrefaction conditions of wood biomass under air and oxy-fuel combustion atmospheres, J. Energy Inst. 93 (2020) 889–898, https://doi.org/10.1016/j.joei.2019.08.001.
[75] N. Agnihotri, G.K. Gupta, M.K. Mondal, Thermo-kinetic analysis, thermodynamic parameters and comprehensive pyrolysis index of Melia azedarach sawdust as a genesis of bioenergy, Biomass Convers. Biorefin. (2022), https://doi.org/10.1007/s13399-022-02524-y.
[76] X. Tian, L. Dai, Y. Wang, Z. Zeng, S. Zhang, L. Jiang, X. Yang, L. Yue, Y. Liu, R. Ruan, Influence of torrefaction pretreatment on corncobs: A study on fundamental characteristics, thermal behavior, and kinetic, Bioresour. Technol. 297 (2020), 122490, https://doi.org/10.1016/j.biortech.2019.122490.
[77] S.R. Naqvi, R. Tariq, Z. Hameed, I. Ali, S.A. Taqvi, M. Naqvi, M.B.K. Niazi, T. Noor, W. Farooq, Pyrolysis of high-ash sewage sludge: Thermo-kinetic study using TGA and artificial neural networks, Fuel 233 (2018) 529–538, https://doi.org/10.1016/j.fuel.2018.06.089.
[78] A. Petrovič, S. Vohl, T. Cenčič Predikaka, R. Bedoić, M. Simonič, I. Ban, L. Čuček, Pyrolysis of Solid Digestate from Sewage Sludge and Lignocellulosic Biomass: Kinetic and Thermodynamic Analysis, 9642, Characterization of Biochar, Sustainability 13 (2021), https://www.mdpi.com/2071-1050/13/17/9642.
[79] R. Kaur, P. Gera, M.K. Jha, T. Bhaskar, Pyrolysis kinetics and thermodynamic parameters of castor (Ricinus communis) residue using thermogravimetric analysis, Bioresour. Technol. 250 (2018) 422–428, https://doi.org/10.1016/j.biortech.2017.11.077.